ISBN: 978-3-95450-205-9 doi:10.18429/JACoW-Cyclotrons2019-MOP004

BEAM DYNAMICS SIMULATION OF THE EXTRACTION FOR A SUPERCONDUCTING CYCLOTRON SC240*

Z. Wu, University of Science and Technology of China, Hefei, China
K. Z. Ding†, J. J. Li, Y. T. Song
Institute of Plasma Physics, Chinese Academy of Sciences, Hefei, China
Z. Wang, Hefei CAS Ion Medical and Technical Devices Co. Ltd., Hefei, China

Abstract

In order to diversify the company's cyclotron, a design study has been carried out on a 240 MeV superconducting cyclotron SC240 for proton therapy, which is based on our experience in design of SC200. In order to increase turn separation and extraction efficiency, resonant precessional extraction method is employed in the extraction system. A first harmonic field consistent with the Gaussian distribution is added to introduce beam precessional motion. Its effects on phase space evolution and turn separation increase is studied by a high efficiency beam dynamics simulation code. According to the study, its amplitude and phase have been optimized to meet the requirements of extraction beam dynamics. Based on beam dynamics simulation, the parameters of extraction system elements (two electrostatic deflectors and six magnetic channels) are chosen. Besides, the effects of sectors spiral direction on beam extraction are studied. Extraction efficiencies and beam parameters have been calculated.

INTRODUCTION

In order to diversify the proton therapy cyclotron product series, ASIPP (Institute of Plasma Physics, Chinese Academy of Sciences) starts designing a superconducting cyclotron to extract 244 MeV, 500 nA proton beam [1]. The main parameters of SC240 cyclotron are listed in Table 1. In order to increase extraction efficiency and decrease the voltage of deflectors as much as possible, the proposed extraction method is resonance extraction [2].

BEAM PRECESSION DESIGN

Working Diagram

Figures 1 and 2 show that Qr drops quickly in extraction region. The beam will cross $Qr = 1$ resonance line when energy reaches 241 MeV. A first harmonic field bump will be added near $Qr = 1$ to increase coherent radial oscillation to generate big turn separation at entrance of first deflector.

Sector Spiral Direction

Before setting about designing the first harmonic field bump, we should choose an optimal sector spiral direction. As shown in Fig. 3, there are two different sector spiral direction: Case 1: beam moves in the direction of the sector spiral, and the position of entrance of first deflector is $\varphi = 44°$; Case2: beam moves against the direction of the sector spiral, and the position of entrance of first deflector is $\varphi = 91°$. We did beam precession simulation in extraction region under the 2 cases above with same amplitude of first harmonic field bump and optimal bump phase. The simulation conditions and results are shown in Fig. 4. The simulation shows that the extraction radius of case 1 is about 1.5 cm bigger than case 2.

Table 1: The Main Parameters of the Cyclotron SC240

Parameter	Value
Extracted beam energy	244 MeV
Extraction radius	80.88 cm
Extraction mechanism	Resonance crossing and precessional motion
Spiral angle (maximum)	71°
Pole radius	84 cm
Outer radius of yoke	160 cm
Hill/valley gap	5 cm/60 cm
Central field/Extraction field	2.39/3.01 T
Coil cross section	dx82×dy115 mm^2
Current density	62.56 A/mm^2
Number of cavity	4
RF frequency	72.79 MHz
Harmonic mode	2
Cavity voltage	~100 kV

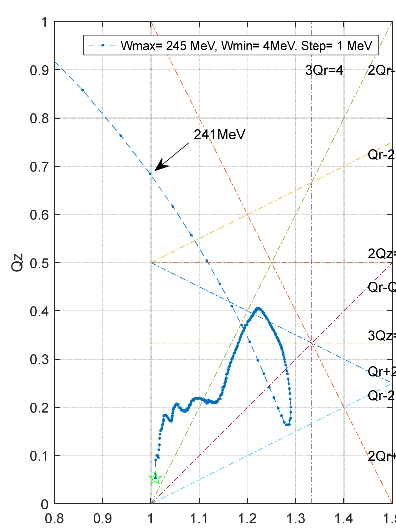

Figure 1: Working diagram of SC240 cyclotron.

* Work supported by National Natural Science Foundation of China under grant No. 11775258 & 11575237, International Scientific and Technological Cooperation Project of Anhui grant No. 1704e1002207.
† kzding@ipp.ac.cn

ISBN: 978-3-95450-205-9 doi:10.18429/JACoW-Cyclotrons2019-MOP004

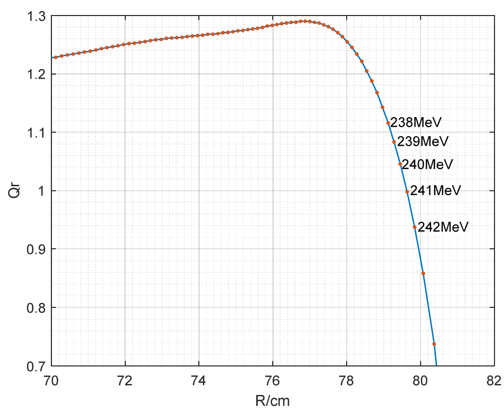

Figure 2: Qr vs. R at extraction region.

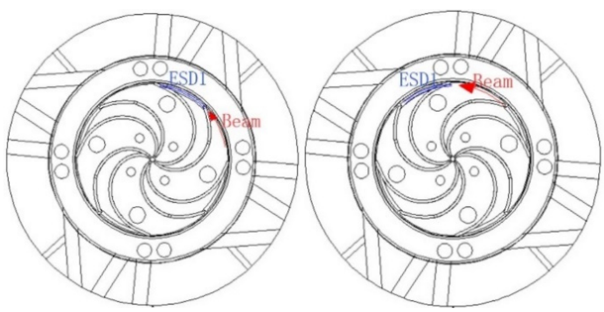

Figure 3: Two different spiral direction of sectors: left-Case1, right-Case2.

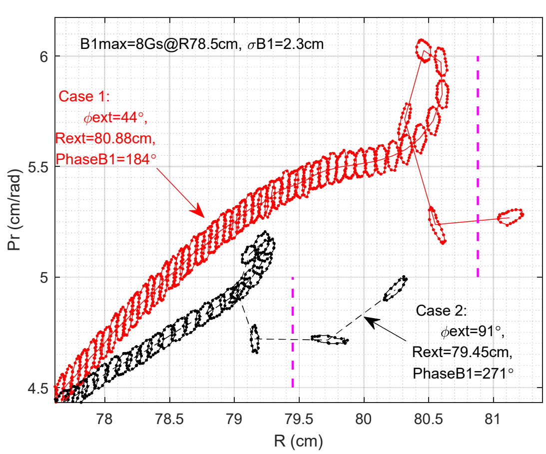

Figure 4: Different spiral direction make different extraction radius.

And the radial impulse at entrance of first deflector of case 1 is about 0.25 cm/rad bigger than case 2. Therefore, we can draw the conclusion that it's easier to deflect the beam in case 1 than in case 2. So we use the sectors whose spiral is in the same direction as the particle motion (case 1) to design beam extraction.

First Harmonic Field Bump

A suitable first harmonic field bump is designed to introduce desirable beam precession. The radial distribution of amplitude of first harmonic field is shown in Fig. 5. The radial distribution of the amplitude is consistent with the Gaussian distribution with a maximum amplitude equal to 8 Gs at center position $Rc = 78.5$ cm, and a width $\sigma = 2.3$ cm. After comparing the beam precession induced by first harmonic bumps with different phase, we found that the optimal phase of first harmonic is $\varphi = 184°$when the entrance of first deflector is at $\varphi = 44°$.

With this first harmonic distribution shown in Fig. 5, we can observe the precession near extraction shown in Fig. 6. The simulation in Fig. 6 is done from 200 MeV, and the initial beam radial phase ellipse has emittance $\varepsilon_r \sim 0.3$ π·mm·mrad. Besides, the central proton is on AEO (accelerating equilibrium orbit). As shown in Figure 6, the turn separation increases about 5 mm due to the first harmonic bump.

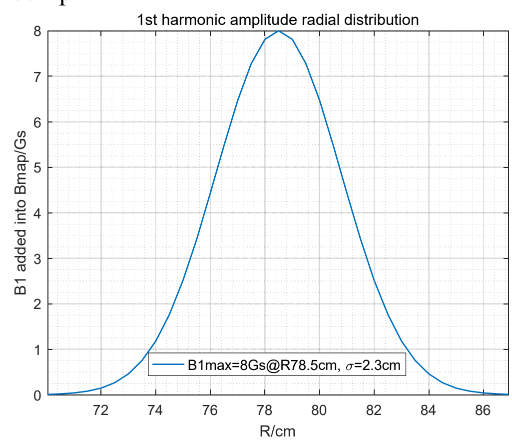

Figure 5: Radial distribution of amplitude of 1st harmonic field.

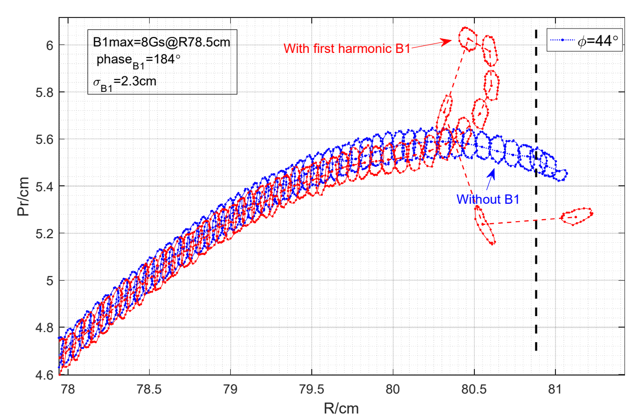

Figure 6: Radial phase space at extraction region.

Main Acceleration Region Simulation

The parameters of initial beam used for main acceleration region beam simulation is that: 1000 protons generated randomly in a phase ellipse around 200 MeV AEO with radial emittance, $\varepsilon_r \sim 0.3$ π·mm·mrad, and longitudinal emittance, $\varepsilon_z \sim 0.4$ π·mm·mrad, phase width = ±5° and energy spread = ±0.165%.

The axial profile of beam is shown in Fig. 7. From the radial phase space (Fig. 6) and the axial profile (Fig. 7), we can see that the optimal radial position of entrance of first deflector' septum is 80.88 cm. Then we can get the beam's parameters at the entrance of first deflector, which is shown in Figure 8. All of the 1000 protons at 200 MeV AEO are accelerated to the entrance of first deflector successfully.

ISBN: 978-3-95450-205-9 doi:10.18429/JACoW-Cyclotrons2019-MOP004

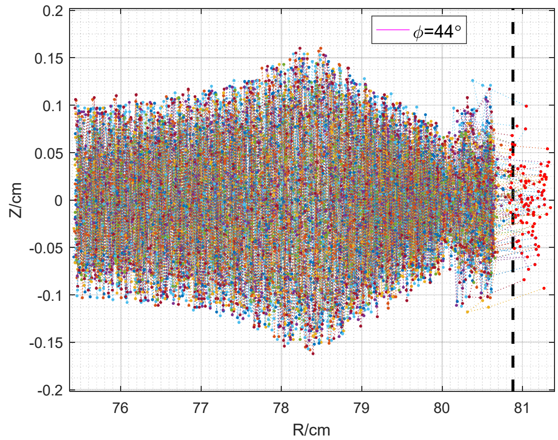

Figure 7: Axial profile of the beam.

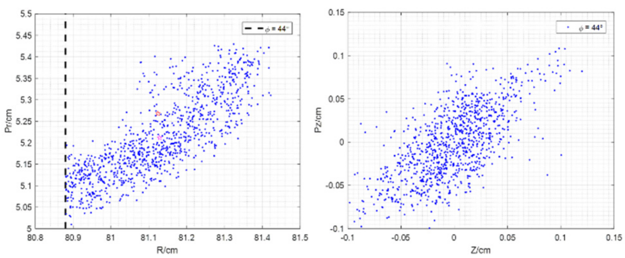

Figure 8: Position of protons on different planes at deflector entrance (Wave = 244 MeV).

EXTRACTION SYSTEM DESIGN

Extraction Trajectory and Envelop

There are two steps to design the extraction system. Firstly, based on the central proton at the entrance of first deflector, we design the radial component of electric field *Er* in deflectors and magnetic field response ΔB in channels to get a suitable central extraction trajectory. Secondly, we design suitable magnetic field gradient based on multi-particle beam simulation with all of the protons at the entrance of first deflector to make beam envelope as small as possible.

The plan view of central extraction trajectory and extraction elements are shown in Figure 9. The geometry and field parameters of all elements are shown in Table 2 and Table 3. There are 2 deflectors placed at the adjacent hills and 6 passive magnetic channels in the extraction system. Electric field strength in deflectors does not exceed 110 kV/cm, gradients of magnetic field in channels are in a range of 2–3 kGs/cm. Five channels focus the beam in horizontal direction. MC4 and edge magnetic field focus the beam in vertical direction. As shown in Fig. 10, the beam envelop at exit of cyclotron (R = 160 cm) does not exceed 5 mm in both horizontal and vertical direction. Figure 11 shows the parameters of extracted beam at the external radius of yoke (R = 160 cm) when the initial beam at 200 MeV AEO has emittance $\varepsilon_r \sim 0.3\ \pi\cdot$mm$\cdot$mrad and $\varepsilon_z \sim 0.4\ \pi\cdot$mm$\cdot$mrad. The output beam at R = 160 cm has emittance $\varepsilon_x = 7.81\ \pi\cdot$mm$\cdot$mrad, $\varepsilon_z = 1.01\ \pi\cdot$mm$\cdot$mrad, average energy = 244 MeV and energy spread = ±0.25%.

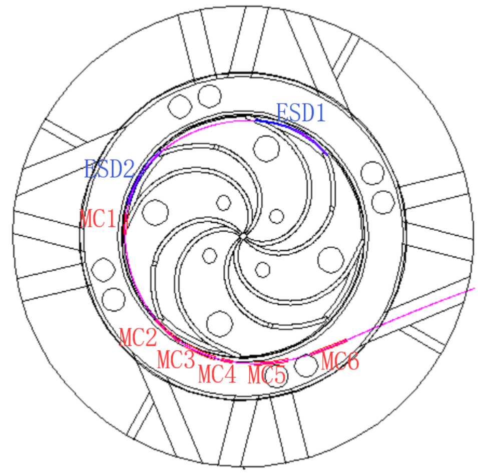

Figure 9: Plan view of extraction system and central extraction trajectory.

Table 2: Geometry Parameters of MCs and ESDs

Element	φ1 (°)	φ2 (°)	Xc (cm)	Yc (cm)	Rc (cm)
MC1	169	179	-3.181	3.568	78.935
MC2	224	239	-0.384	-8.181	77.974
MC3	242	257	4.734	-0.471	87.261
MC4	260	265	7.134	7.258	95.376
MC5	275	290	8.194	25.809	114.012
MC6	300	315	-41.92	181.892	278.180
ESD1	44	84	6.103	12.092	68.479
ESD2	134	164	-11.26	4.209	71.000

Table 3: Field Parameters of MCs and ESDs

Element	ΔB (kGs)	dB/dx (kGs/cm)
MC1	-0.5	2.5
MC2	-0.2	2.5
MC3	-0.2	2.5
MC4	-0.2	-2.0
MC5	-0.2	3.2
MC6	-0.2	3.2
ESD1		Er = 110 kV/cm
ESD2		Er = 100 kV/cm

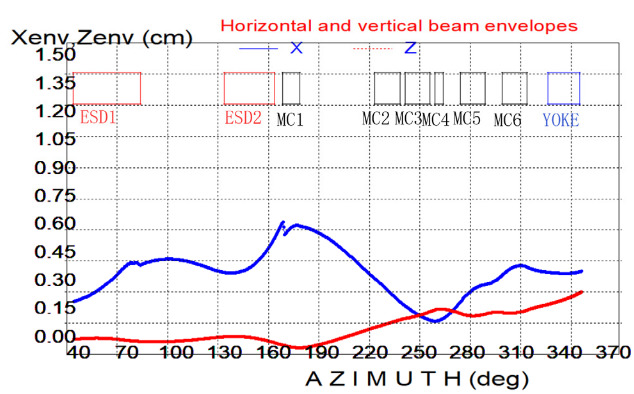

Figure 10: Beam envelop in extraction system.

ISBN: 978-3-95450-205-9 doi:10.18429/JACoW-Cyclotrons2019-MOP004

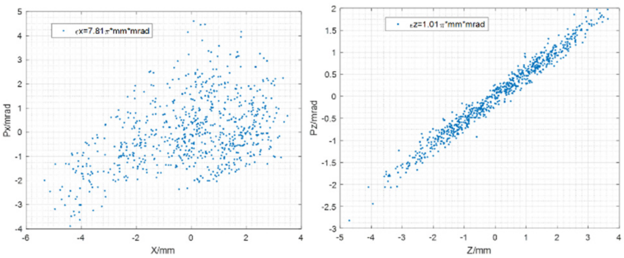

Figure 11: Beam parameters at the exit of cyclotron (R=160 cm).

Beam Loss and Efficiency

The distribution of beam loss is given in Table 4. The protons are mainly lost on ESD1 and MC1 in horizontal direction. The extraction efficiency achieves 76.4%.

Table 4: Beam Loss Distribution in Extraction System

Lost on ESD1	Lost on MC1	Extracted
11.7%	11.9%	76.4%

CONCLUSION

It is easier to deflect beam in a resonance extraction system when the sector's spiral is in the same direction as the particle motion. We have generated a 5 mm turn separation by adding an 8 Gs 1st harmonic bump near $Qr = 1$. In addition to 2 electrostatic deflectors, the proposed extraction system contains 6 sets of passive magnetic channels. The extracted beam envelop is less than 5 mm and extraction efficiency is about 76.4%.

REFERENCES

[1] F. Jiang *et al.*, "Design study of a compact superconducting cyclotron SC240 for proton therapy", in *Proc. IPAC'19*, Melbourne, Australia, May 2019, pp. 3506-3509. doi:10.18429/JACoW-IPAC2019-THPMP029

[2] T. I. Arnette, H. G. Blosser, M. M. Gordon, and D. A. Johnson, "Cyclotron programs for a small computer", *Nucl. Instrum. Methods*, vol. 18-19, pp. 343-345, 1962. doi:10.1016/S0029-554X(62)80044-5